

Electron Microscopy I

Lecture 08

TT.Prof. Dr. Yolita M. Eggeler

Laboratory for electron microscopy,
CFN building, 2nd floor, room 215

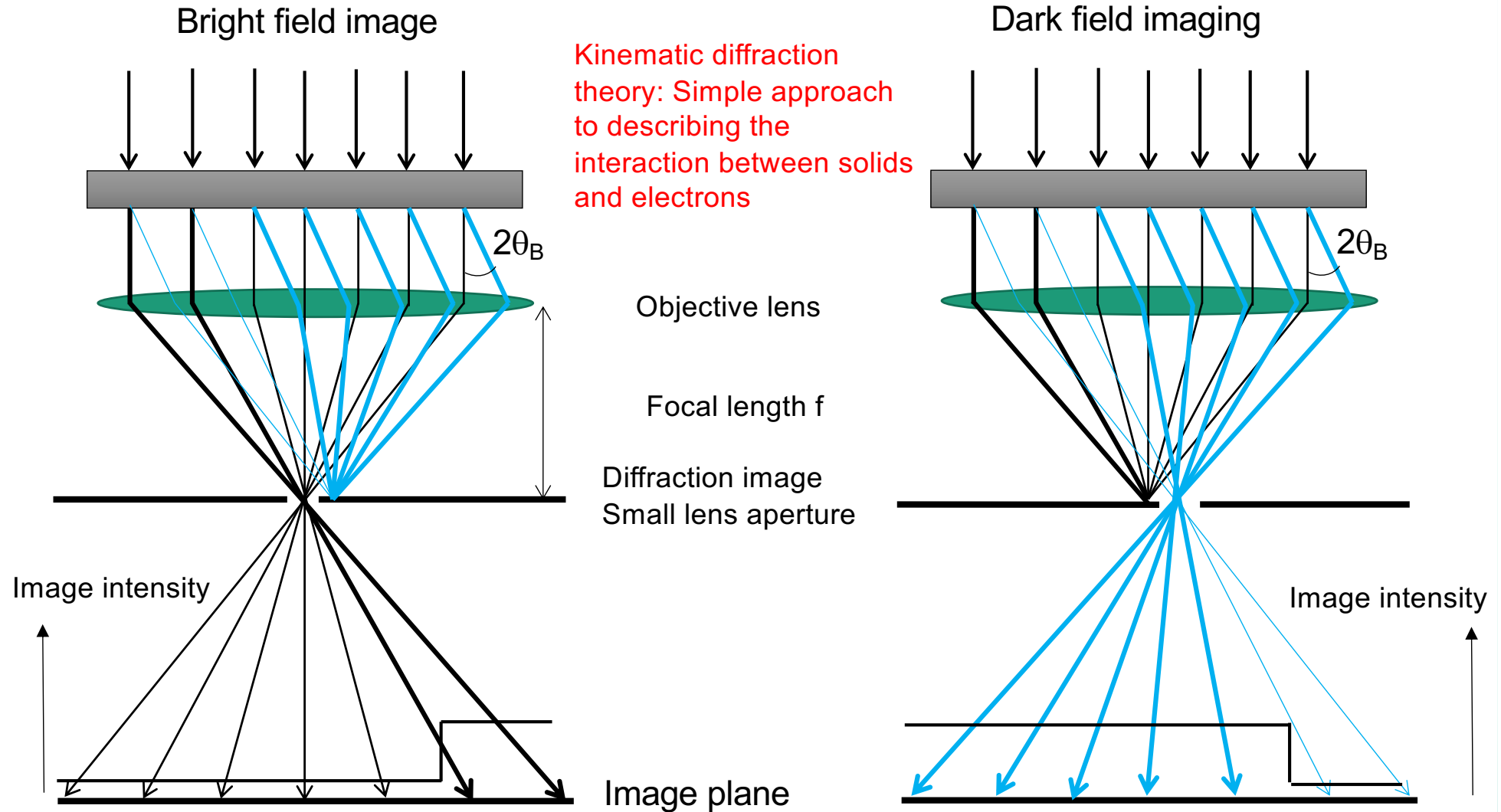
yolita.eggeler@kit.edu

Phone 608-43724

1. From light microscopy to electron microscopy
2. Practical aspects of transmission electron microscopy (TEM) and scanning transmission electron microscopy (STEM)
3. **Electron diffraction in solids: kinematic diffraction theory**
 - 3.1 Interaction of electrons with individual atoms
 - 3.2 Interaction of electrons with crystalline objects: Kinematic diffraction theory
- 4. Contrast formation (conventional TEM and STEM) and practical examples of imaging objects in solid state and materials research**
 - 4.1 Mass thickness contrast
 - 4.2 Column approximation
 - 4.3 Contrasts in perfect (single) crystals
 - 4.4 Contrast in crystals with lattice defects, moirée effect
5. Dynamic electron diffraction
6. Imaging of the crystal lattice/high-resolution electron microscopy (HRTEM)
- ~~7. Scanning transmission electron microscopy~~
8. Electron holography
9. Transmission electron microscopy with phase plates

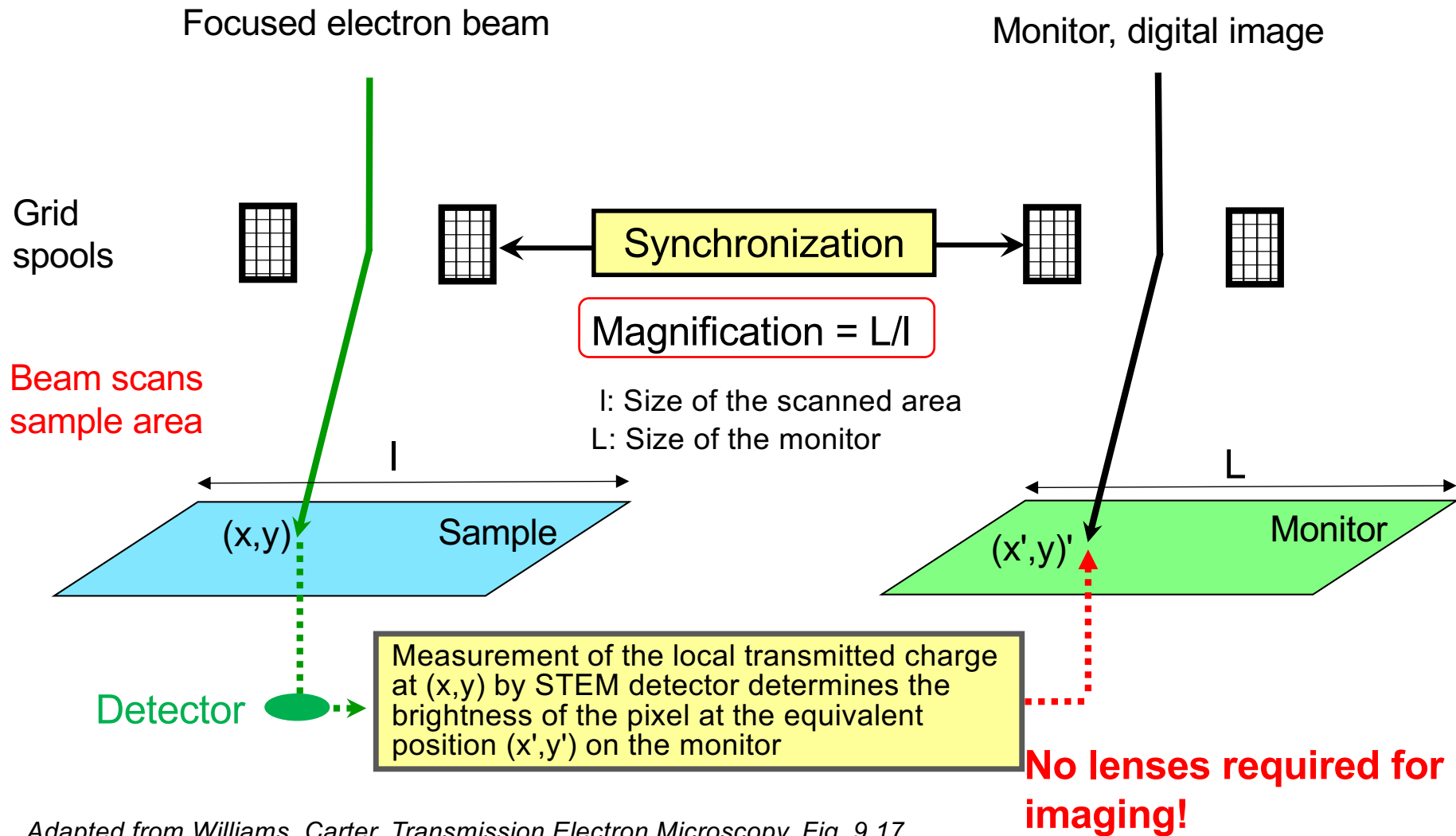
4. Contrast formation (conventional TEM and STEM) and examples the imaging of objects in solid state and materials research

Conventional bright field and dark field imaging



4. Contrast formation (conventional TEM and STEM) and examples the imaging of objects in solid state and materials research

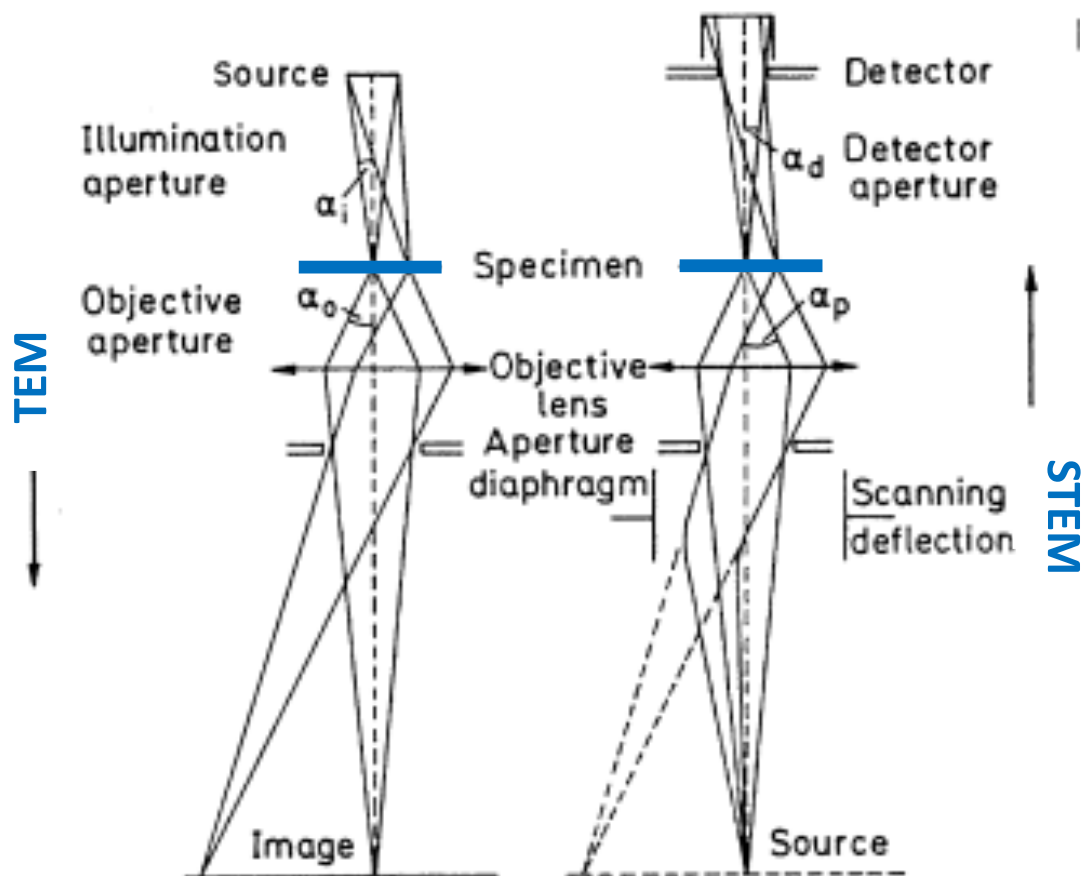
Scanning transmission electron microscopy (STEM) in the transmission electron microscope: Principle of image formation



Adapted from Williams, Carter, Transmission Electron Microscopy, Fig. 9.17

4. Contrast formation (conventional TEM and STEM) and examples the imaging of objects in solid state and materials research

The reciprocity theorem describes conditions under which STEM and TEM
Illustrations show identical contrast



TEM:

Illumination of the sample with small Beam convergence angle α_i (0.1 - 1 mrad)

Figure: Lens aperture $\alpha_o > 3$ mrad significantly larger as α_i

STEM:

Illumination of the sample with a focused beam (large beam convergence angle α_p)

Figure: Detection by bright field detector with small detection angle range α_d

Equal contrast of brightfield TEM and brightfield STEM images when

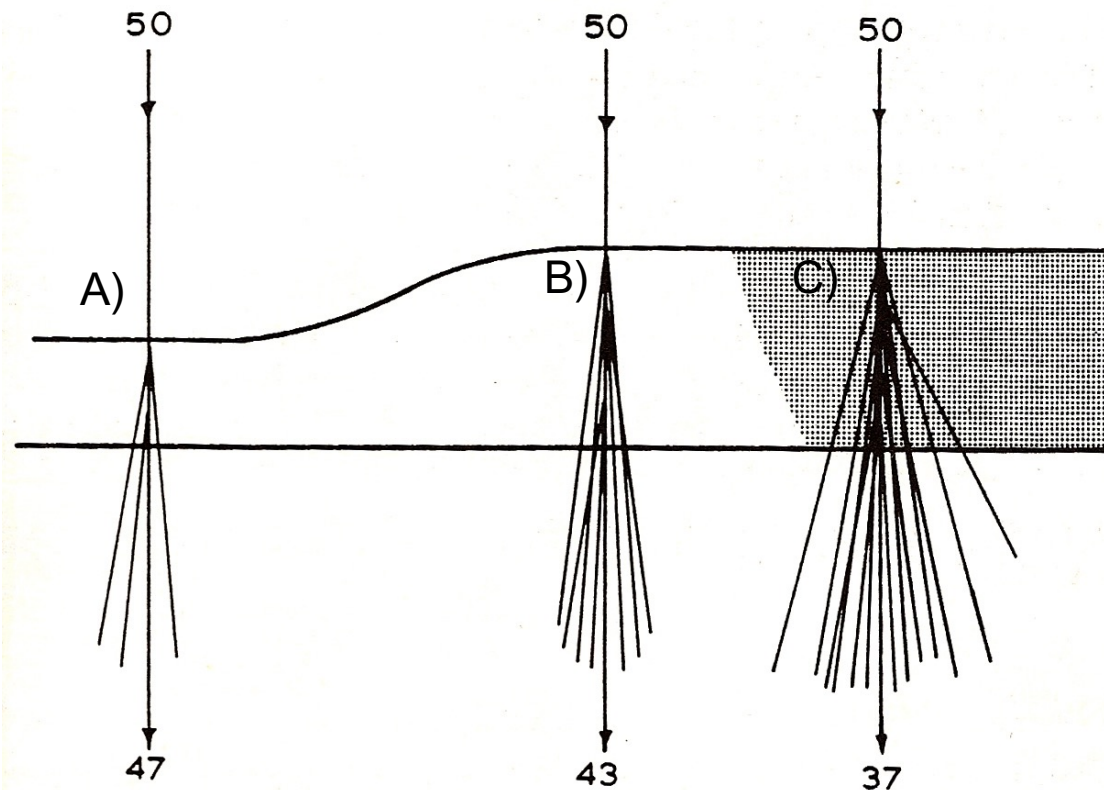
$$\alpha_i = \alpha_d \text{ and } \ll \alpha_o = \alpha_p$$

L. Reimer, H. Kohl, Transmission Electron Microscopy, Fig. 4.20

Extension to dark field (S)TEM and high resolution resolving phase contrast images possible

4.1 Mass thickness contrast

Mass thickness contrast in objects **with amorphous structure and crystalline objects without strongly excited Bragg reflexes ("kinematic diffraction conditions")**

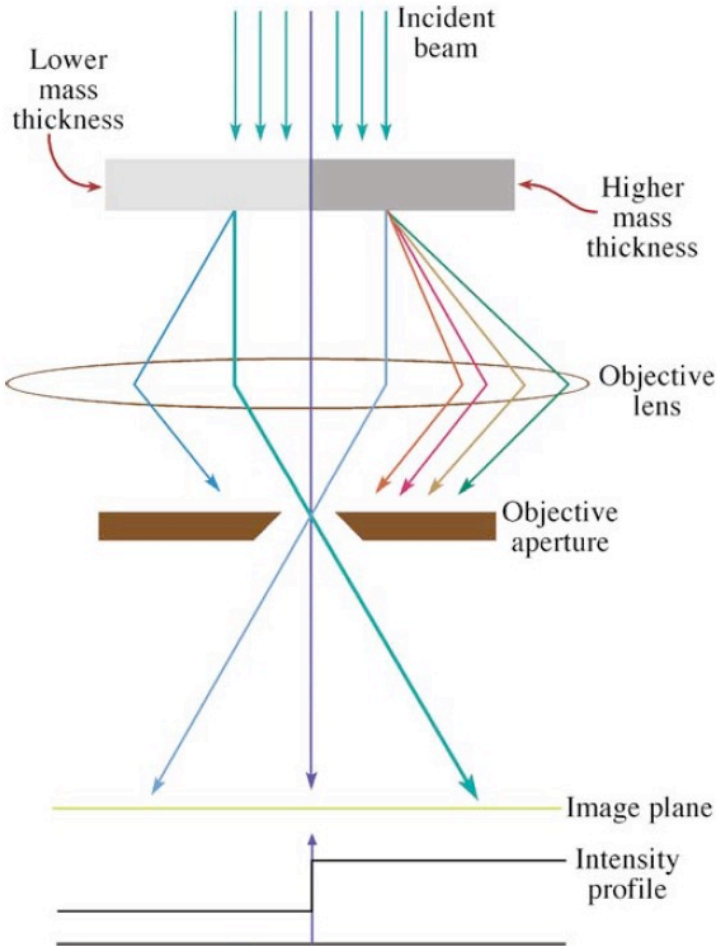


Goodhew, Humphreys, Beanland, " Electron Microscopy and Analysis ", Fig. 4.9

Electron scattering in different areas of a thin sample

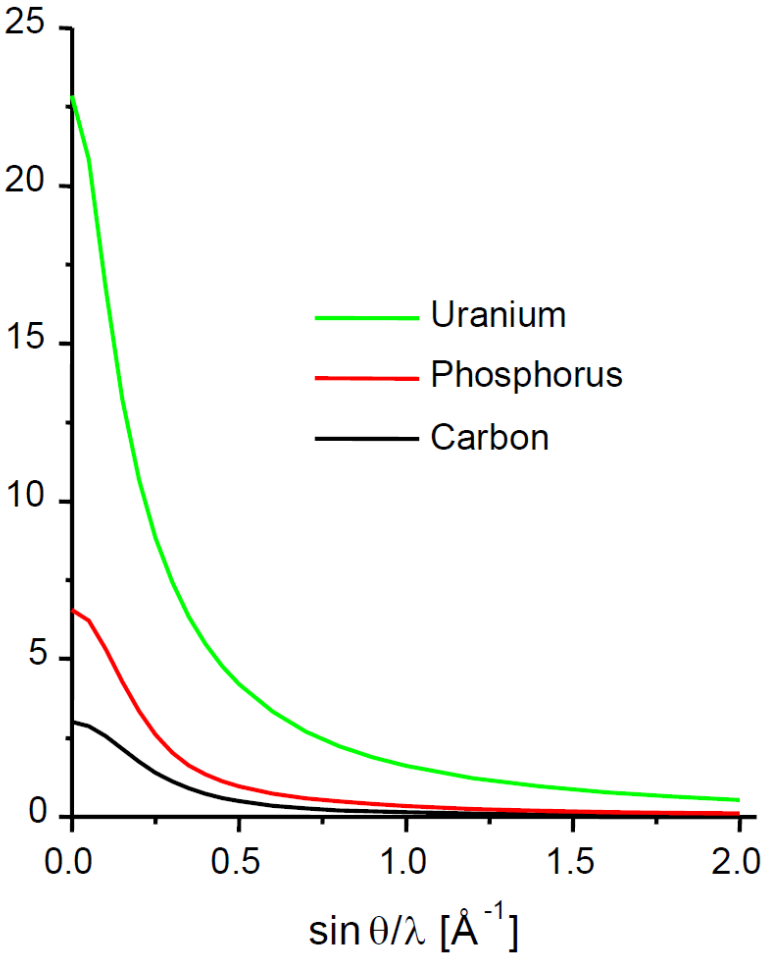
- A) Scattering of a few electrons in thin sample areas
- B) Scattering of a larger number of electrons with increasing sample thickness
- C) In the range of the same thickness but higher density, the scattering is even greater

4.1 Mass thickness contrast



Carter&Williams , Transmission Electron Microscopy, Figure 22.4

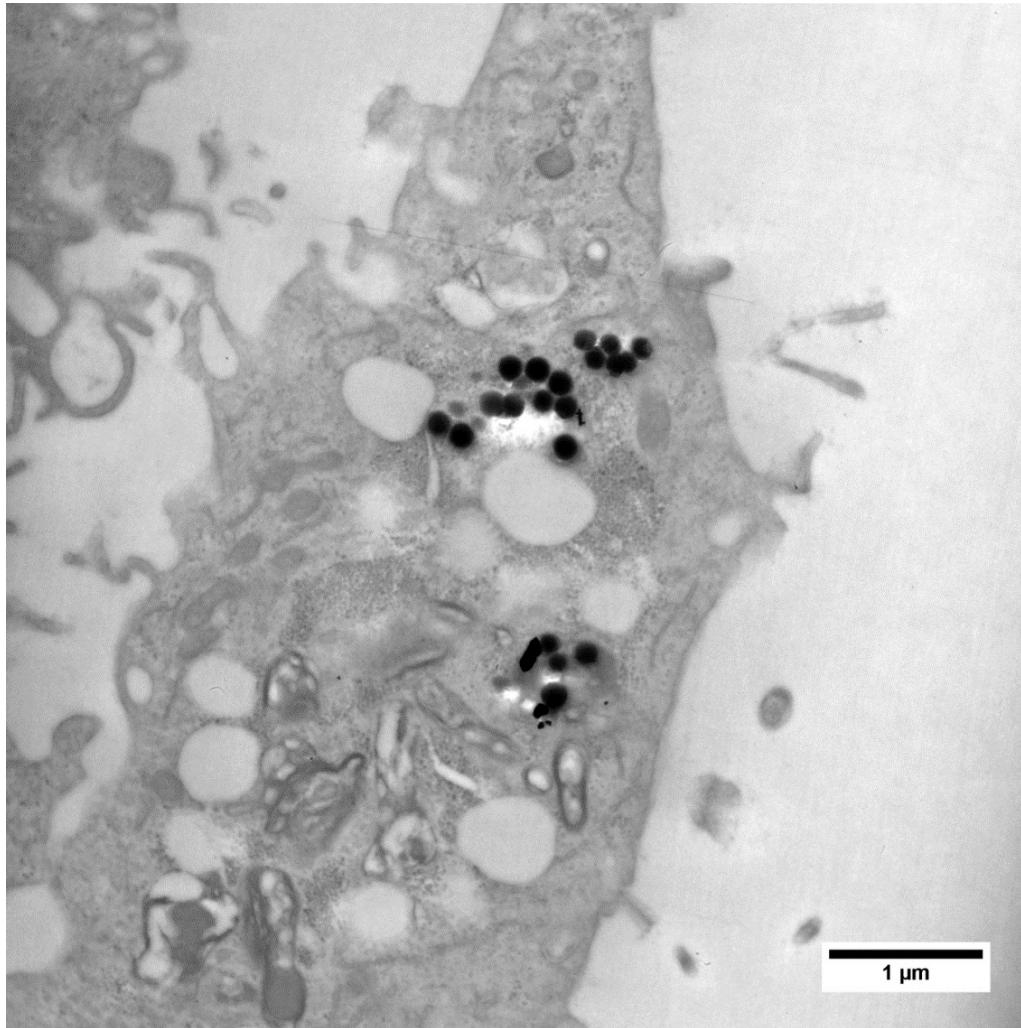
Atomic scattering factor [\AA]



Atoms with a high atomic number scatter more strongly.

4.1 Mass thickness contrast

Mass thickness contrast in biological objects with amorphous structure

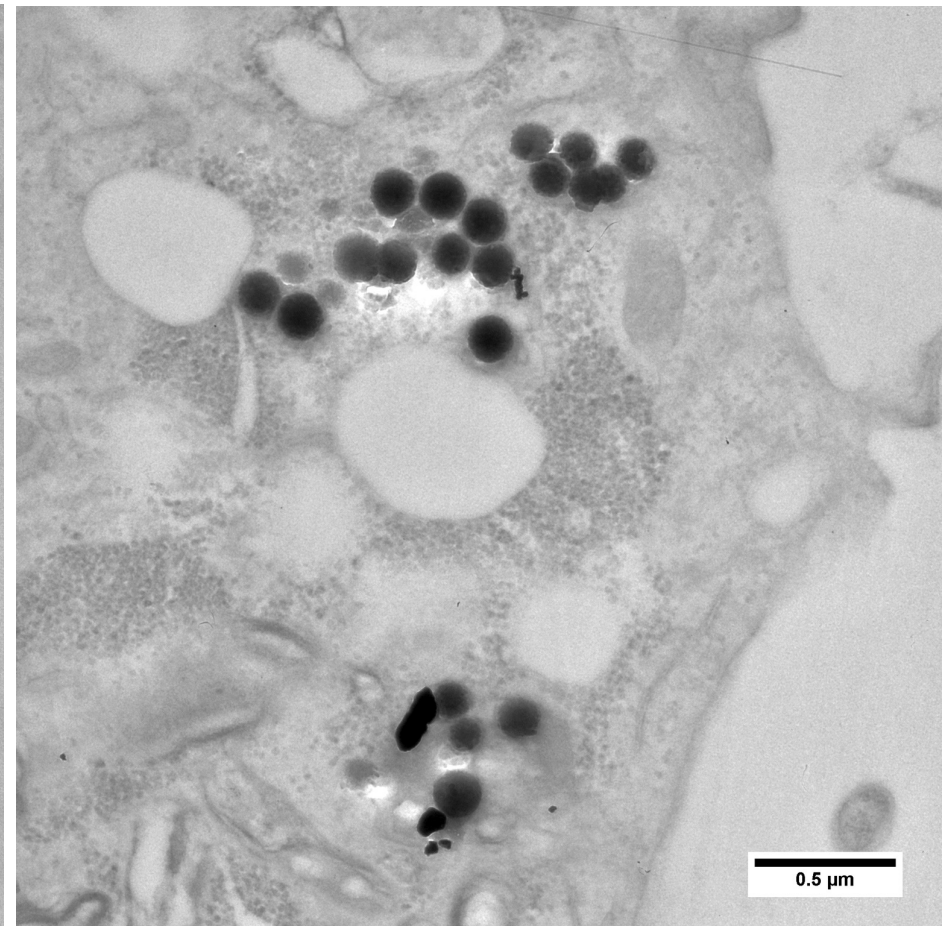
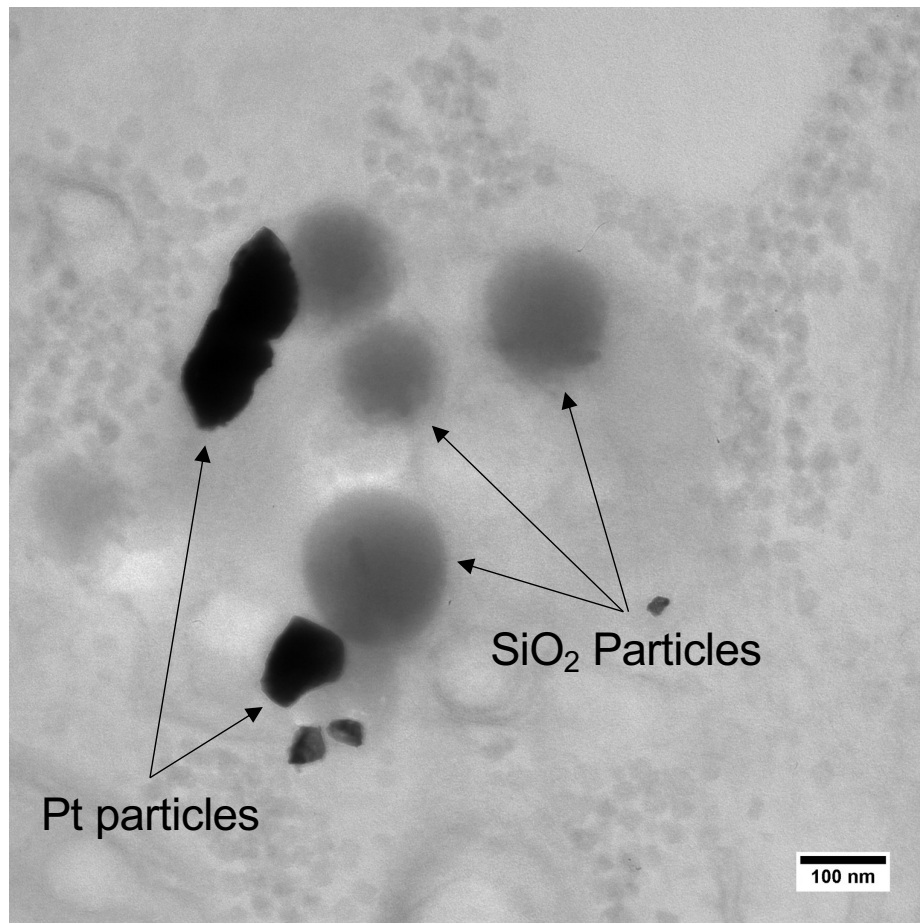


H. Blank (LEM)

HT29 Intestinal carcinoma cell with SiO_2 - and Pt nanoparticles: TEM bright field image of a thin section with *homogeneous* thickness → Image brightness determined by local material density

4.1 Mass thickness contrast

Mass thickness contrast in biological objects with amorphous structure

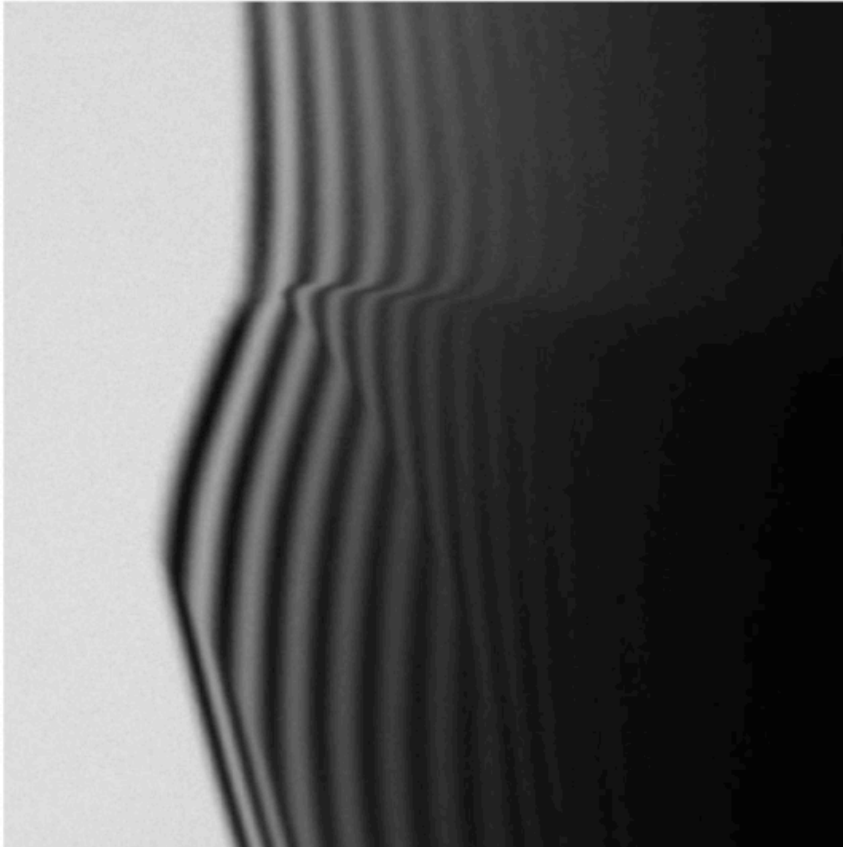


HT29 Intestinal carcinoma cell with SiO₂ - and Pt nanoparticles:
TEM bright field image

H. Blank (LEM)

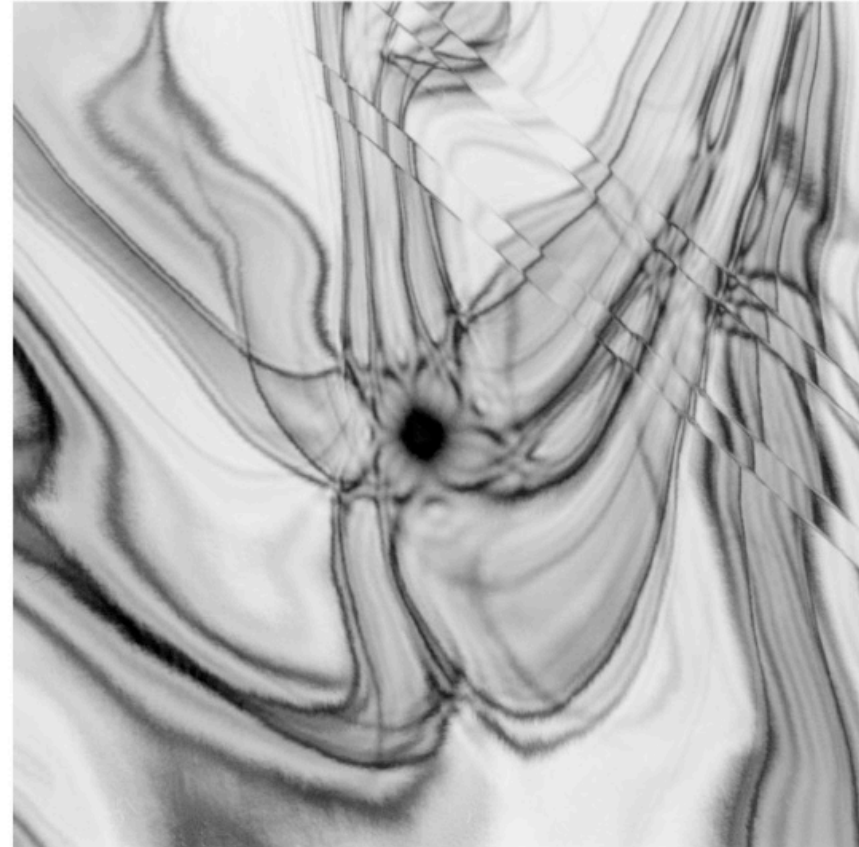
4.3 Contrasts in perfect crystals

Thickness contours



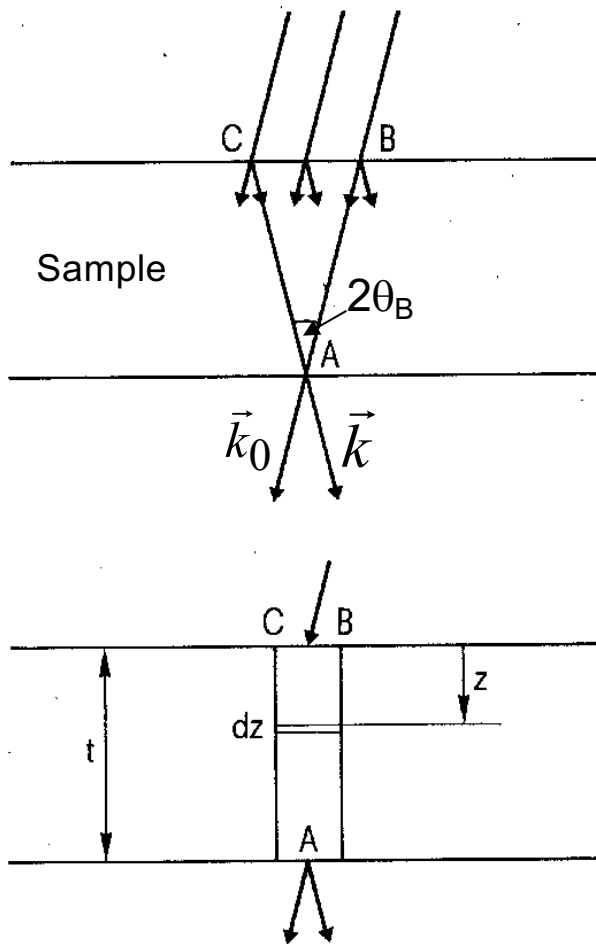
Bright field image of a wedge-shaped edge of a crystalline sample.

Bending contours



Bright field image of a bent crystalline foil.

4.2 Column approximation



Fuchs, Oppolzer, Rehme "Particle Beam Microanalysis", Fig. 4.30

Calculation of image intensity for conventional TEM images - (only one reflex for image)

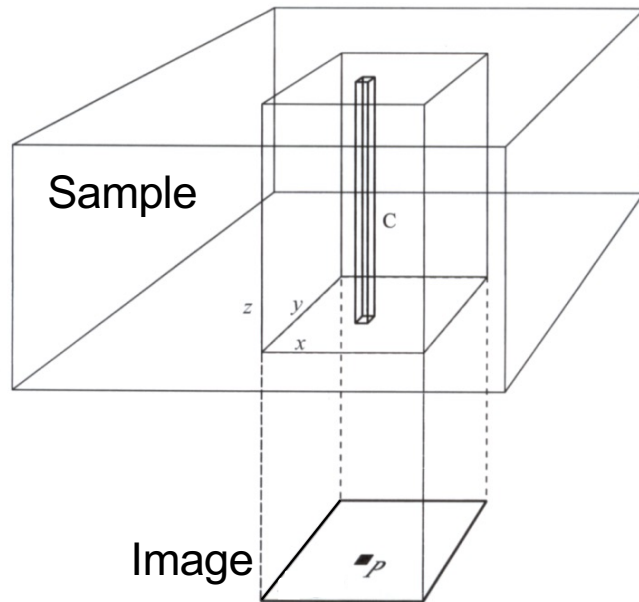
- Image contrast for TEM *bright field imaging*: Intensity of the zero beam at the bottom of the sample as a function of the sample location (x,y) (Intensity of the *Bragg reflex* I_g for *dark-field images*)
- Simplification through two-beam **conditions**
Observation of the intensity of the Bragg reflex

$$I_g \propto |F|^2 = |G|^2 |F_s|^2$$

Zero beam intensity $I_o = 1 - I_g$
(intensity of the incident electron beam normalized to 1)

- Calculation of the local image intensity:
Observation of the amplitudes of the zero beam and the Bragg reflex at point A on the underside of the sample: only contribution from I_o and I_g in the CBA triangle
- Replace the acute triangle with a **column** (in 3 dimensions) with $d \approx \frac{CB}{2}$
(for 100 nm sample thickness and $\theta_B < 1^\circ$, the size of the column in x and y direction is ≈ 1 nm)

4.2 Column approximation



Goodhew, Humphreys, Beanland,
"Electron Microscopy and Analysis",
Fig. 4.19



- In neighboring columns: Intensities under two-beam conditions (I_g and thus I_o) are independent of each other to a good approximation
- Column dimensions very small
Approximation: Sample composed of many columns
- Image composed of "pixels" $I(n_x, n_y)$
- → Pixel corresponds to one column
- good description of conventional TEM images

Calculation of the intensity of each column:

- Calculation of I_g and I_o for each column using kinematic (or dynamic) diffraction theory for the relevant sample thickness, imaging vector \vec{g} and excitation error \vec{s}
- Assumption: Column is part of a plate that extends infinitely in the x and y directions
(otherwise very broad diffraction reflections perpendicular to the column)


4.3 Contrasts in perfect crystals

Calculation of the amplitude of a Bragg reflex (kinematic theory):

By integrating the lattice amplitude over the sample thickness t

$$G \propto \int_0^t \exp(2\pi i s_z z) dz$$

With constant excitation error s_z


$$I_g = F_S^2 G^2 \propto F_S^2 \frac{\sin^2(\pi s_z t)}{(\pi s_z)^2}$$

(structure factor independent of thickness)

Note: constant excitation error rarely fulfilled in practice due to bending of thin TEM specimens

4.3 Contrasts in perfect crystals

$$I_g = F_S^2 G^2 \propto F_S^2 \frac{\sin^2(\pi S_z t)}{(\pi S_z)^2}$$

Contrast/image intensity of a perfect (defect-free) single crystal with constant sample thickness?

A perfect single crystal of constant thickness without any disturbance shows a homogeneous image brightness.

What causes differences in intensity in the image?

Intensity differences, i.e. an image contrast when

1. sample is of varying thickness (often the case in practice)
2. lattice planes change their orientation in relation to the electron beam
(sample bending, polycrystalline sample)
3. in the presence of defects

4.3 Contrasts in perfect (single) crystals

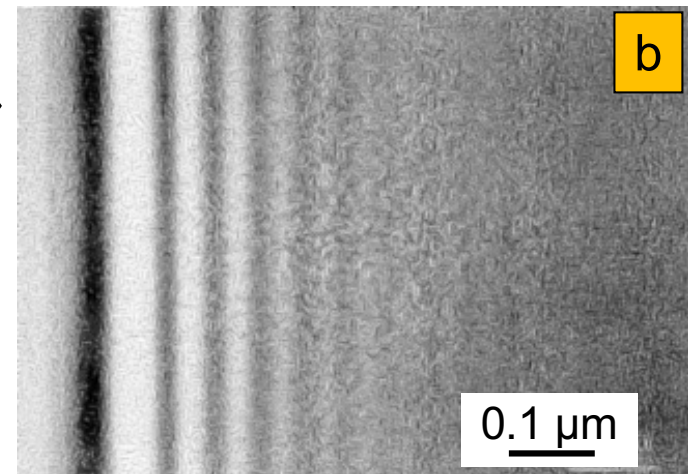
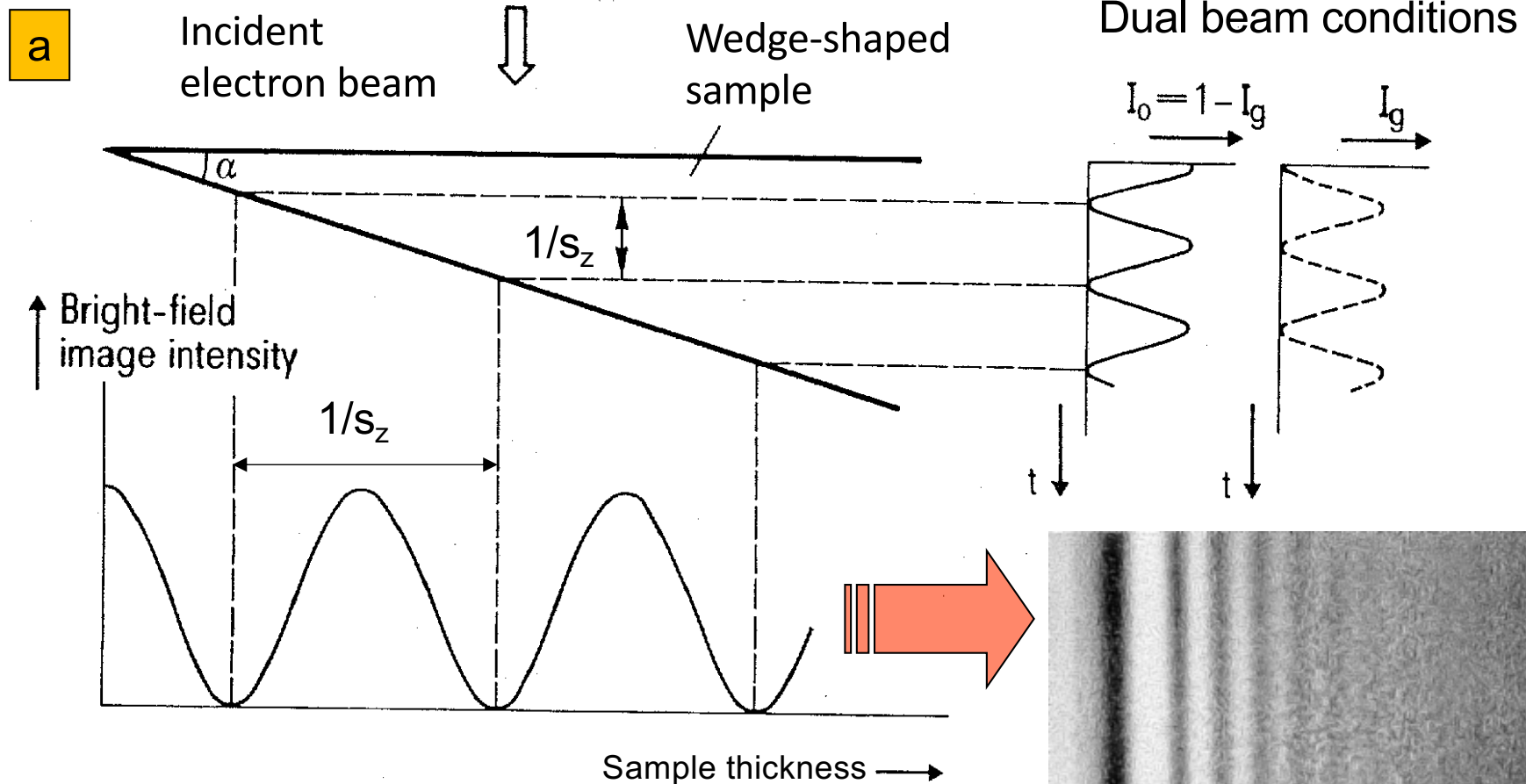


Image taken with $s = 0_z$
 ↑ Sample edge

Fuchs, Oppolzer, Rehme "Particle Beam Microanalysis", p.186

Creation of thickness contours:

- a) schematic representation
- b) Bright field image of a Si single crystal with thickness contours at the edge of a wedge-shaped sample

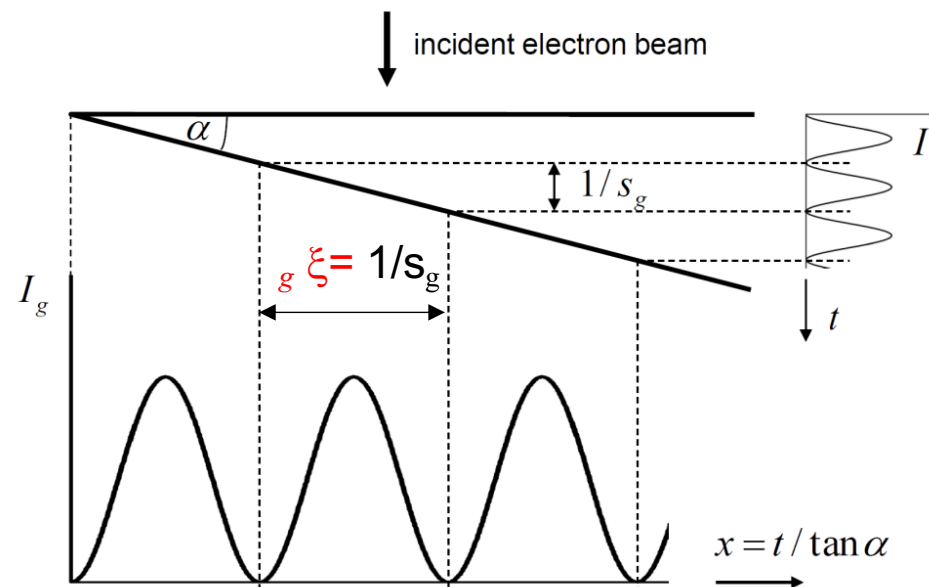
4.3 Contrasts in perfect (single) crystals

Thickness contours

- Sample with wedge-shaped thickness profile: complementary intensity oscillation of excited Bragg reflex I_g and zero beam I_0

Kinematic theory: $I_0 = 0$ for TEM sample thicknesses of $t_n = 1/(2s_z) + n/s_z$

- The parameter $1/s_z$ specifies the change in sample thickness between two zero points of the intensity. The change in sample thickness between two intensity minima (or intensity maxima) is referred to as the **extinction length ξ** .

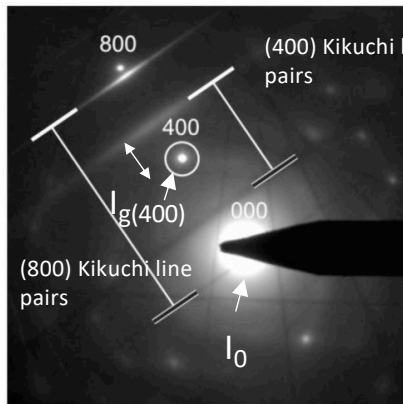


4.3 Contrasts in perfect (single) crystals

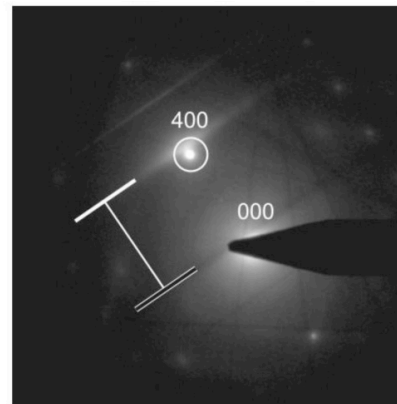
Thickness contours

- The sample thickness at which intensity minima and maxima occur only agrees with the prediction of the kinematic diffraction theory if $|s_z| \gg 0$ and $I_g \ll I_0$.

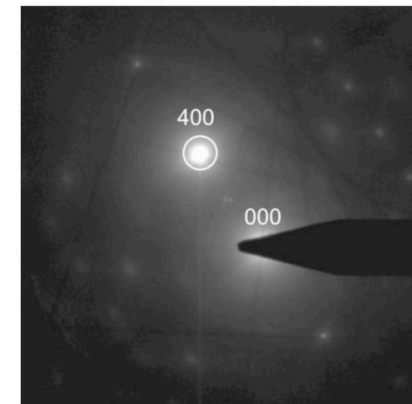
$s_{400} \gg 0$



$s_{400} > 0$

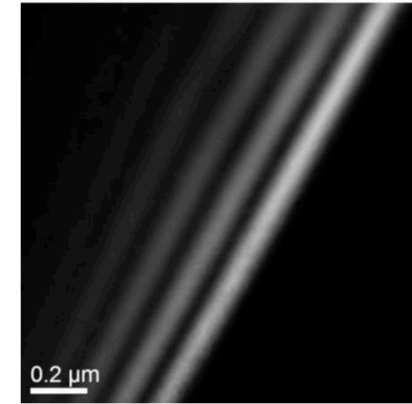
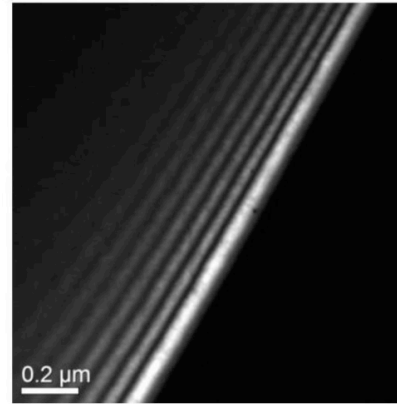
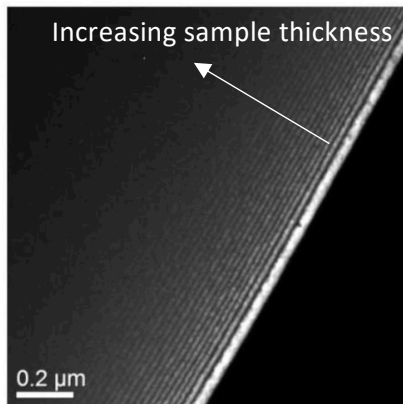


Bragg condition ($s_{400} = 0$)



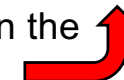
Diffraction image shows the setting of the excitation error $|s_z|$ in the two-beam case.

Increasing sample thickness



Dark-field image shows thickness contours at the edge of a wedge-shaped sample.

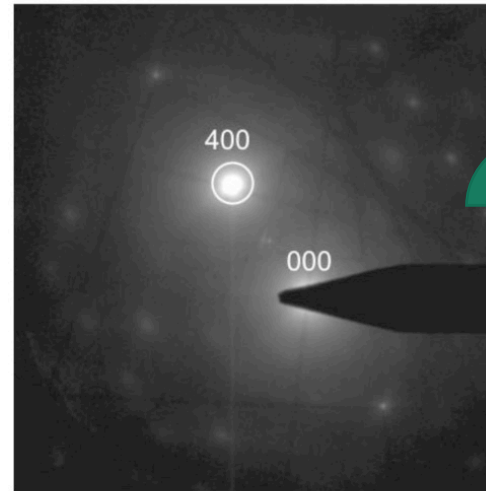
According to the kinematic theory, no thickness contours are expected in the Bragg condition! (→ dynamic theory is required)



4.3 Contrasts in perfect (single) crystals

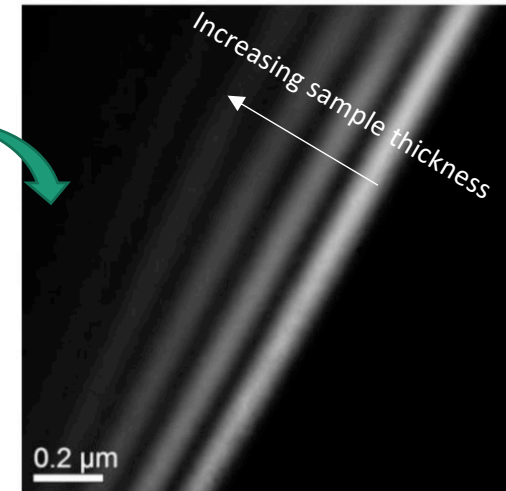
$$I_g = F_S^2 G^2 \propto F_S^2 \frac{\sin^2(\pi s_z t)}{(\pi s_z)^2}$$

Bragg condition ($s_{400} = 0$)



Two-beam drop in Bragg-condition with $s=0$

Dark field imaging



Intensity oscillations

Experimentally observed contrast is in contradiction to kinematic theory

- Intensity oscillations as a function of thickness t : $1/s_z \rightarrow \infty$ for $s_z \rightarrow 0$
- Decreasing contrast of the intensity oscillation with increasing sample thickness

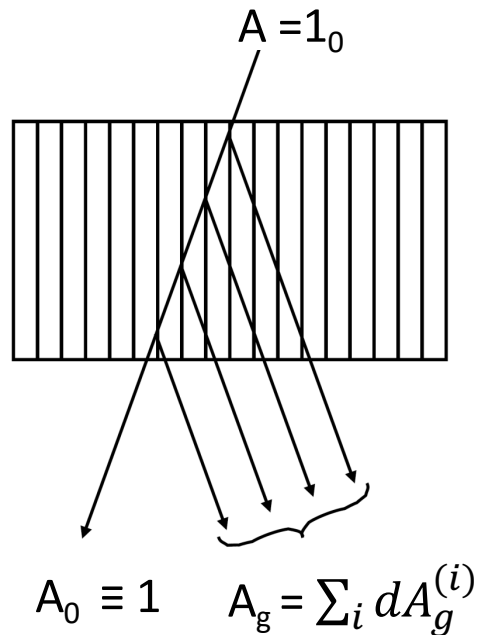


$s_z = 0$ and small s_z : **Application of dynamic diffraction theory necessary**

4.3 Contrasts in perfect crystals

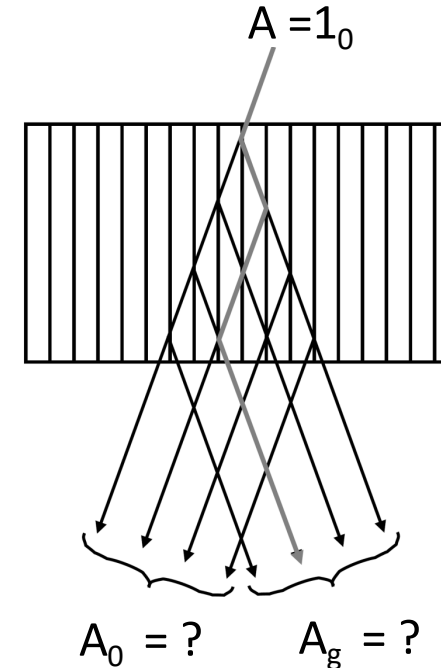
Qualitative differences between kinematic and dynamic diffraction theory

Kinematic diffraction theory



- Amplitude of the zero beam A_0 is constant in good approximation, with increasing specimen thickness
- Only single electron scattering (electrons are only scattered once).
 - Electron losses of the zero beam are neglected.

Dynamic diffraction theory



- $A_0 \neq$ constant with increasing sample thickness
- Increasing intensity of the stimulated Bragg reflex
 - Multiple electron scattering: Electrons are scattered "back" from the Bragg reflex into the zero beam.

4.3 Contrasts in perfect crystals

Result of dynamic diffraction theory (solution of the Schrödinger equation for two-beam conditions using the Bloch threshold approach in Chapter 5):

Formally identical to the result of the kinematic diffraction theory

Replacement of s_z by **effective excitation error** \bar{s}_z

$$I_g \propto F_S^2 \frac{\sin^2(\pi \bar{s}_z t)}{(\pi \bar{s}_z)^2} \quad \text{with} \quad \bar{s}_z = \sqrt{s_z^2 + \frac{1}{\xi_g^2}} \quad \text{with} \quad \xi_g = \frac{\pi V_e \cos\theta_B}{\lambda F_{S,g}} \quad \left(= \frac{h^2}{2\lambda m_{rel} e V_g} \right)$$

Extinction length ξ_g

- λ Electron wavelength
- m_{rel} Relativistic electron mass
- s_z Experimental excitation error (as opposed to effective excitation error \bar{s}_z)
- V_e Volume of the unit cell
- V_g Coefficient of the electrostatic potential for excited reflex \vec{g}
- $F_{S,g}$ Structure factor for the excited Bragg reflex with reciprocal lattice vector
- θ_B Bragg angle for excited Bragg reflex \vec{g}

For $s_z = 0$ (Bragg condition exactly fulfilled): Periodicity of the thickness contours with ξ_g

Typical extinction lengths for electrons with 100 keV to 400 keV: 10 nm – several 100 nm

4.3 Contrasts in perfect (single) crystals

Table 7.1. Extinction distances ξ_g [Å] for elements in a two-beam condition with $s = 0$ (100 keV electrons). [7.1]

| Diffraction | Al | Cu | Ni | Ag | Pt | Au | Pb | Fe | Nb | Si | Ge |
|-------------|------|-----|-----|-----|-----|-----|-----|------|------|------|------|
| 110 | | | | | | | | 270 | 261 | | |
| 111 | 556 | 242 | 236 | 224 | 147 | 159 | 240 | | | 602 | 430 |
| 200 | 673 | 281 | 275 | 255 | 166 | 179 | 266 | 395 | 367 | | |
| 211 | | | | | | | | 503 | 457 | | |
| 220 | 1057 | 416 | 409 | 363 | 232 | 248 | 359 | 606 | 539 | 757 | 452 |
| 310 | | | | | | | | 712 | 619 | | |
| 311 | 1300 | 505 | 499 | 433 | 274 | 292 | 418 | | | 1349 | 757 |
| 222 | 1377 | 535 | 529 | 455 | 288 | 307 | 436 | 820 | 699 | | |
| 321 | | | | | | | | 927 | 4781 | | |
| 400 | 1672 | 654 | 652 | 544 | 343 | 363 | 505 | 1032 | 863 | 1268 | 659 |
| 411 | | | | | | | | 1134 | 944 | | |
| 331 | 1877 | 745 | 745 | 611 | 385 | 406 | 555 | | | 2046 | 1028 |
| 420 | 1943 | 776 | 776 | 634 | 398 | 420 | 572 | 1231 | 1024 | | |

face-centered cubic (fcc)
body-centered cubic (bcc)
Diamond structure

B. Fultz, J.M. Howe, Table 7.1

4.3 Contrasts in perfect (single) crystals

Effective extinction length $\xi_{g,eff}$

$$\xi_{g,eff} = \frac{1}{\bar{s}_z} = \frac{\xi_g}{\sqrt{1 + w^2}} \quad \text{with} \quad w = s_z \xi_g$$

| | |
|-----------------------|----------------------------------|
| $w = s_z \xi_g \gg 1$ | kinematic theory $\xi_g = 1/s_z$ |
| $w = 0$ | dynamic theory ξ_g |
| $0 < w < 5$ | Extinction length given by |

Reduction of contrast with increasing sample thickness

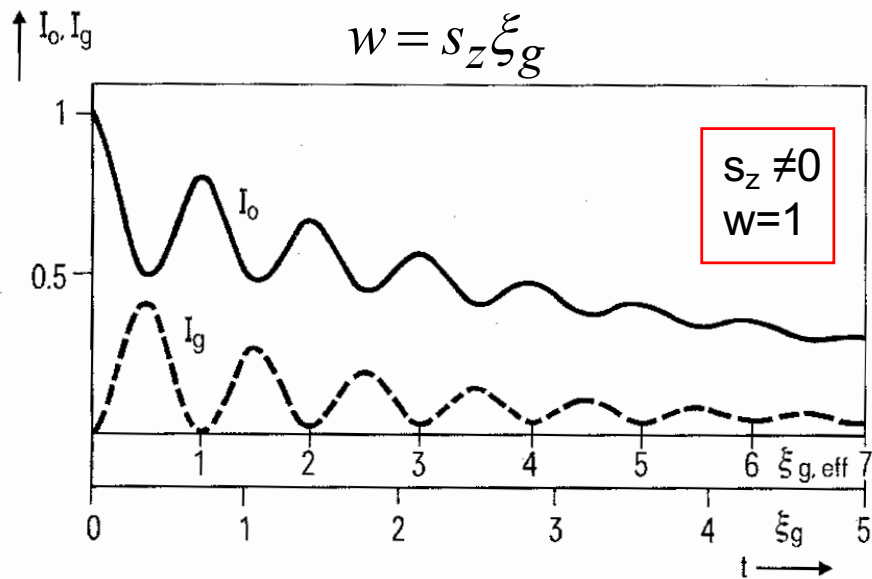
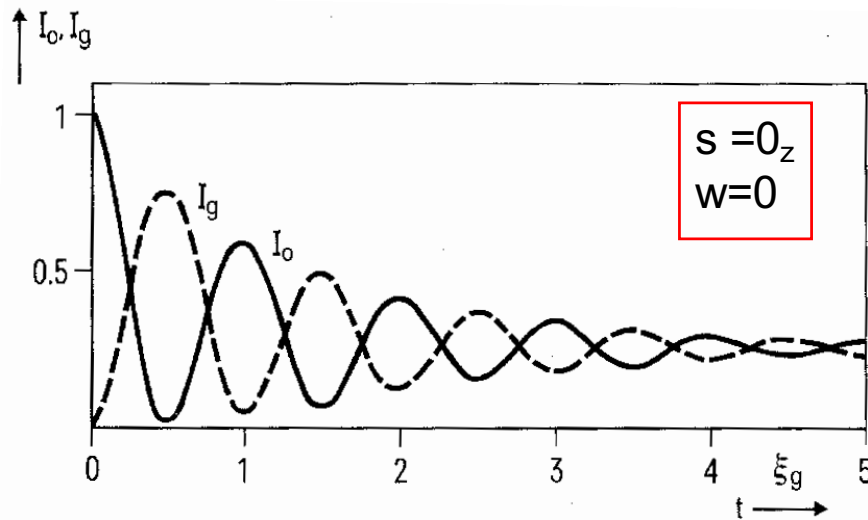
Formal description by complex scattering potential / complex extinction length

$$\frac{1}{\xi_g} \rightarrow \frac{1}{\xi_{g,abs}} = \frac{1}{\xi_g} + \frac{i}{\xi_g''} \quad \text{Typical (empirical) value:} \quad \xi_g'' = 0.1 \xi_g$$

Actual causes of the decrease in intensity in TEM images with increasing sample thickness ("absorption")

- Electrons that are scattered at large angles are suppressed by the lens diaphragm
- Dynamic diffraction theory: different attenuation of Bloch waves

4.3 Contrasts in perfect (single) crystals



Fuchs, Oppolzer, Rehme "Particle Beam Microanalysis", p. 188

Dynamic diffraction theory through
Solution of the Schrödinger equation
for a two-beam case:
Interference of 2 Bloch waves with
slightly different wave
lengths and different
strong damping

$$\xi_{g,eff} = \frac{1}{s_z} = \frac{\xi_g}{\sqrt{1+w^2}}$$

Calculation of the reduction in contrast between
light and dark thickness contours

Fig. 4-35.
Bright-field and dark-field image
intensities I_0 (solid line) and I_g
(dashed line) as a function of
specimen thickness t calculated
by dynamical theory for different
deviation parameters: a) $s = 0$,
b) $s = 1/\xi_g$ ($w = 1$) [4-38]. As in
Fig. 4-33 the curves represent inten-
sity profiles of thickness fringes.

4.3 Contrasts in perfect (single) crystals

Bending contours

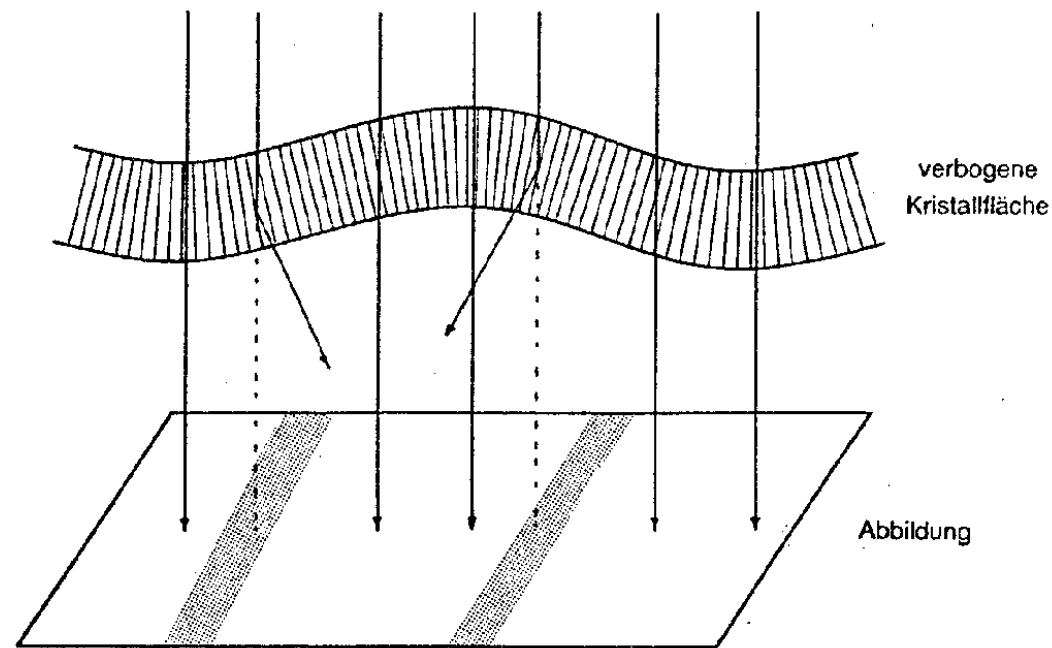


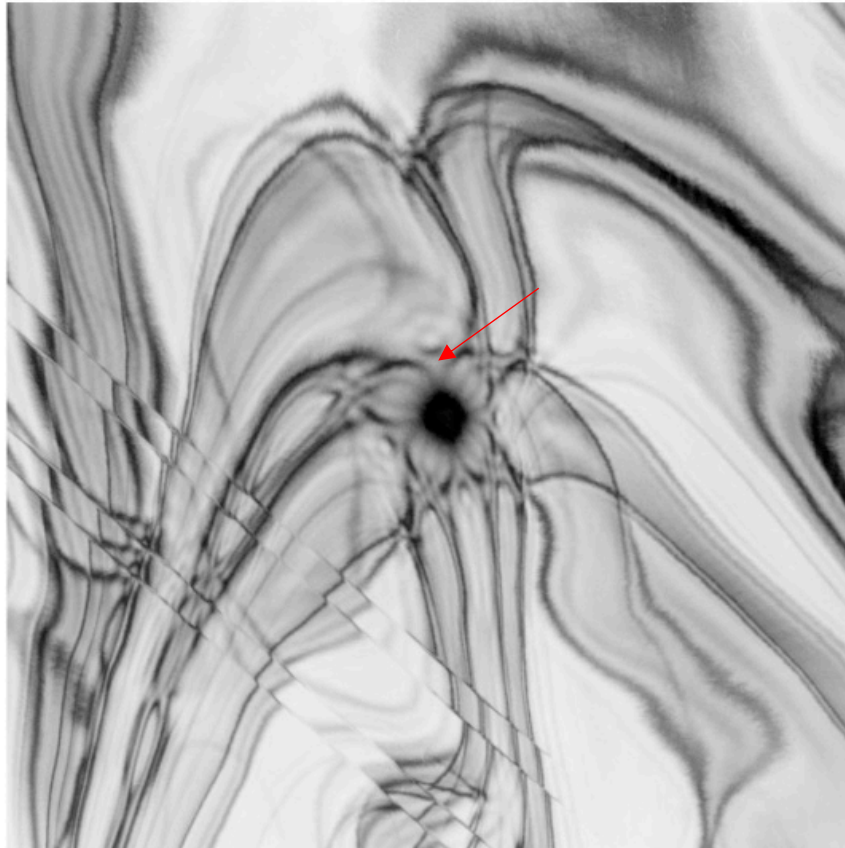
Abb. 4.12 Schematische Darstellung einer verbogenen Einkristallfolie. Das Bild zeigt die Entstehung von Biegelinien in den Bereichen der Folie, deren Orientierung genau der Braggschen Bedingung entspricht.

Goodhew, Humphreys, Beanland, "Electron Microscopy and Analysis", Fig. 4.14

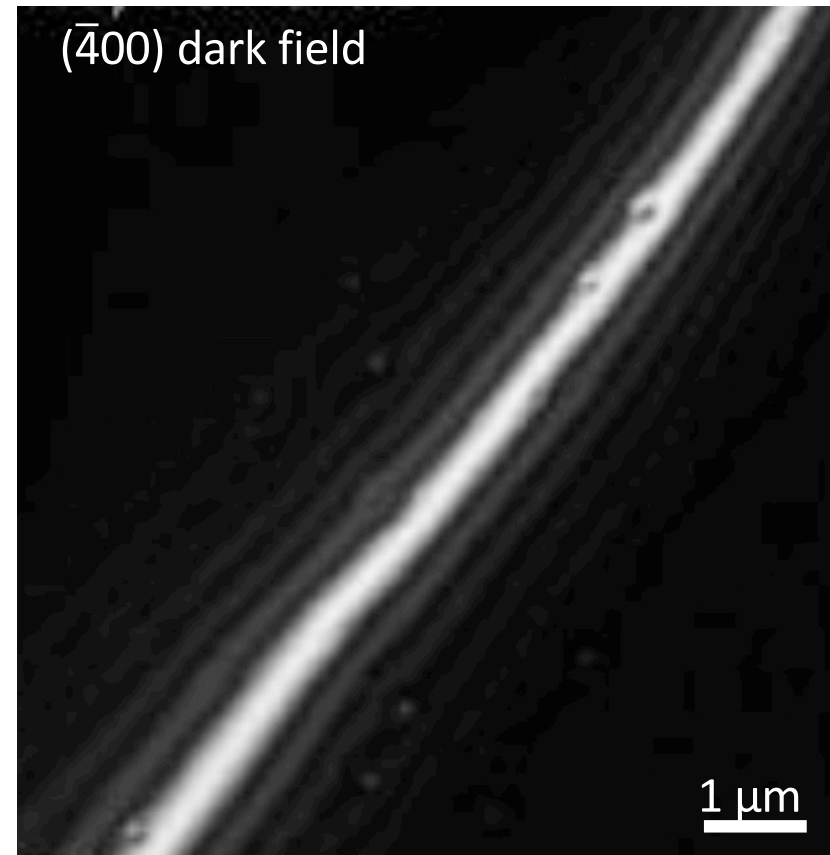
$$I_g \propto \frac{\sin^2(\pi \bar{s}_z t)}{(\pi \bar{s}_z)^2}$$

4.3 Contrasts in perfect (single) crystals: Bending contours

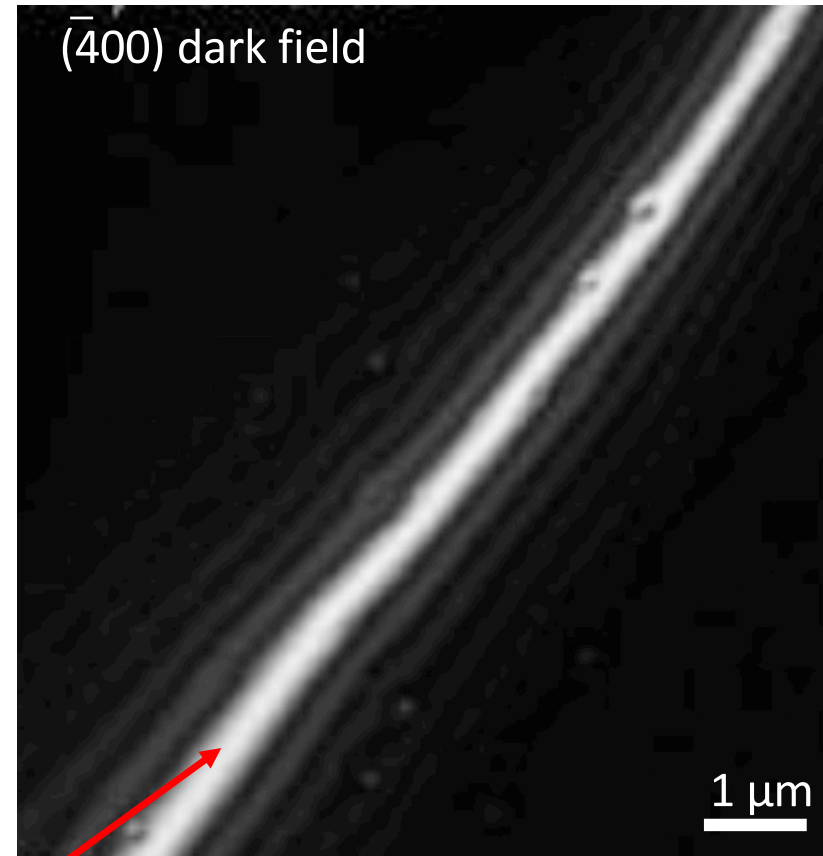
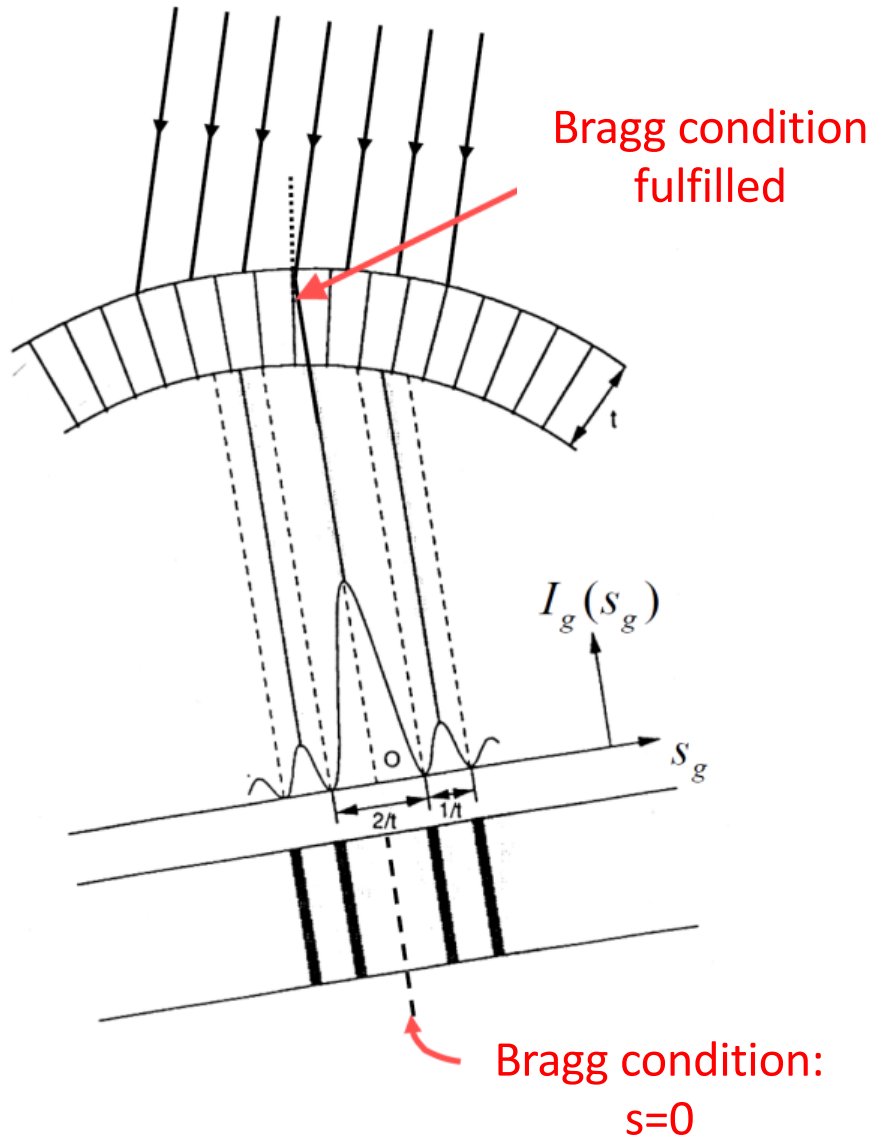
Heavily bent thin foil: bright field image
[100] Zone axis 200 kV



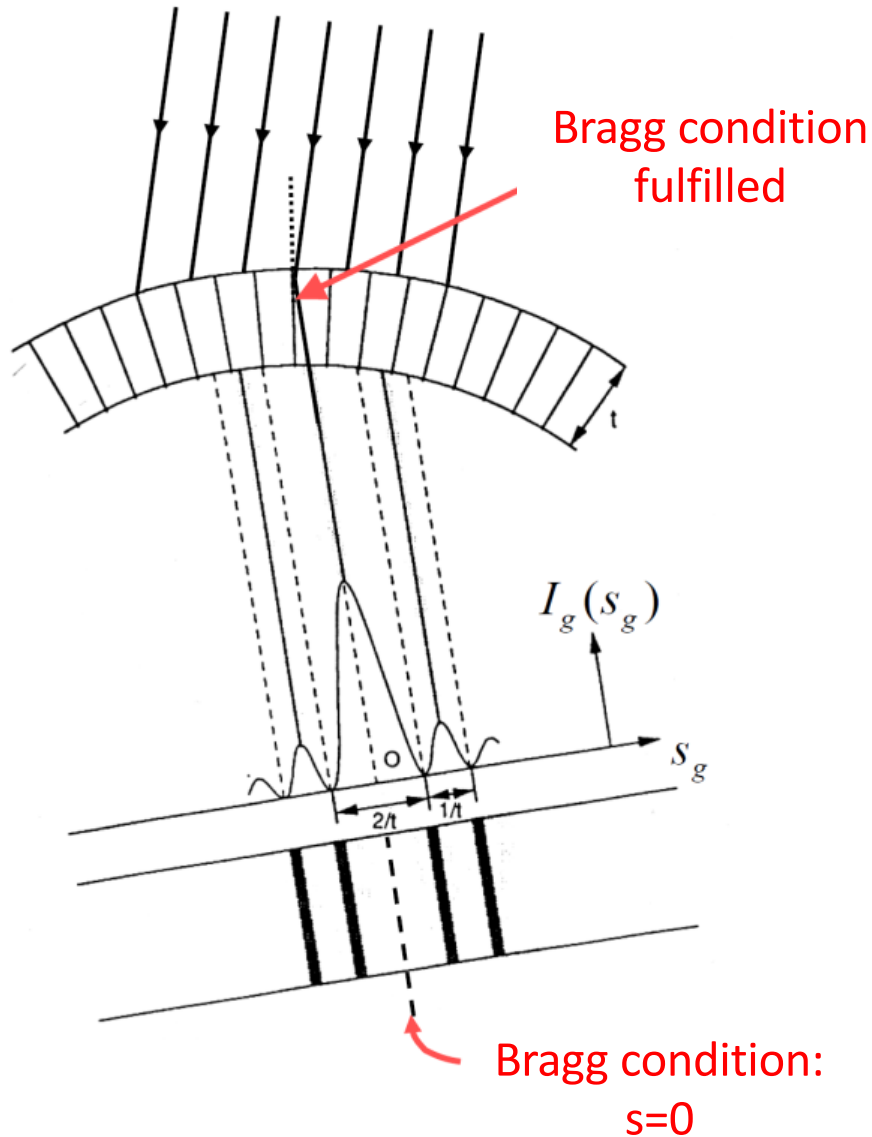
Heavily bent thin foil: bright field image
[100] Zone axis 200 kV



4.3 Contrasts in perfect (single) crystals: Bending contours



4.3 Contrasts in perfect (single) crystals: Bending contours



$$I_g \propto \frac{\sin^2(\pi \bar{s}_z t)}{(\pi \bar{s}_z)^2}$$

for constant t

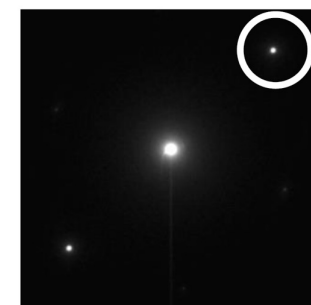
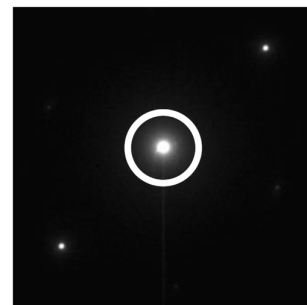
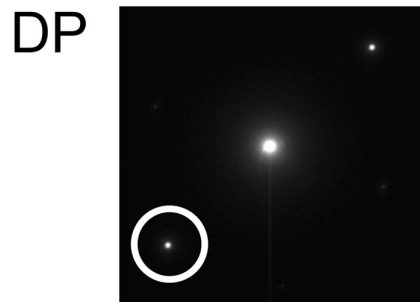
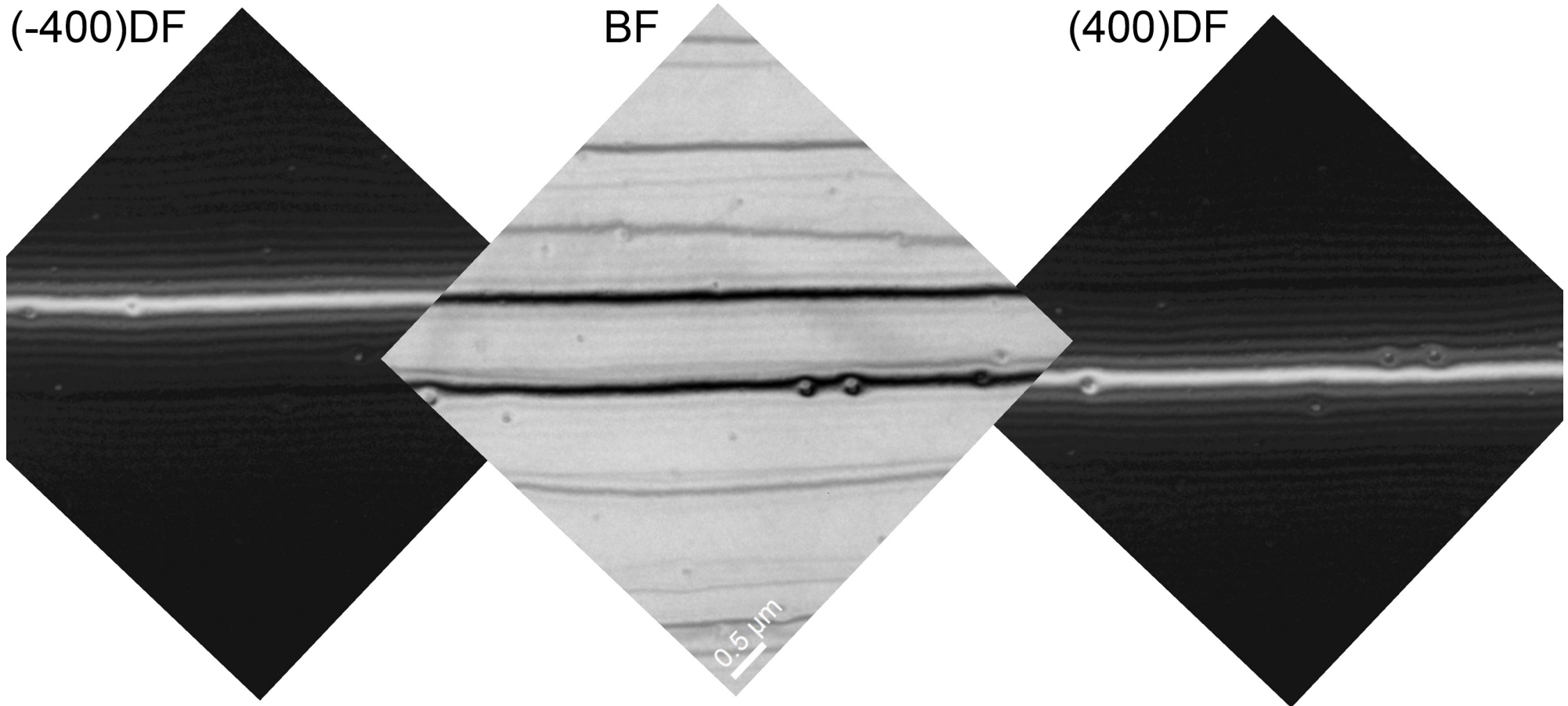
With $\xi_g = \frac{\pi V_e \cos\theta_B}{\lambda F_{S,g}}$ Extinction length of the Bragg reflex g

In kinematic theory, the maximum of the rocking curve is at $s_z=0$, i.e. exactly in the Bragg condition.

The minima (zeros) of the rocking curve / bending contour are enclosed:

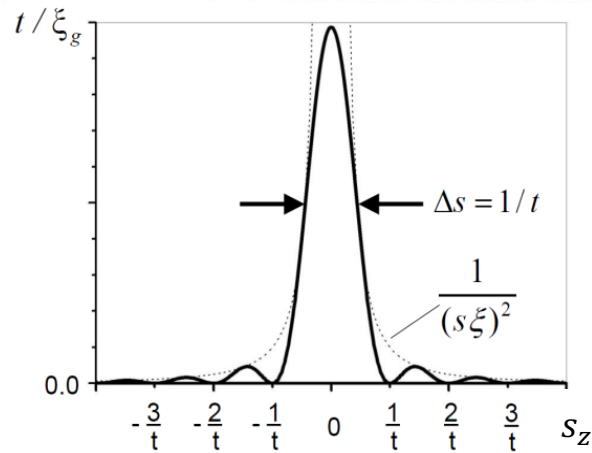
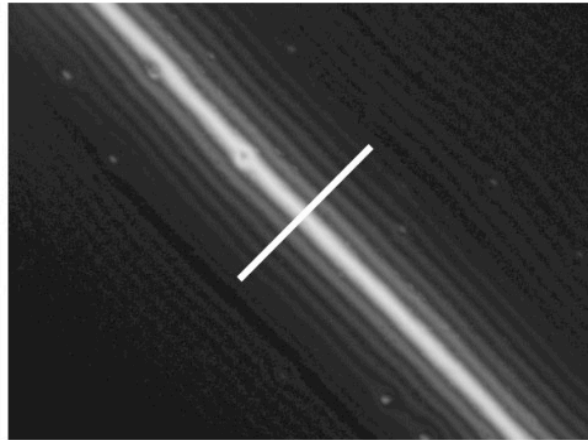
$$s_z = \frac{n}{t}, \quad n = \pm 1, \pm 2, \dots$$

4.3 Contrasts in perfect (single) crystals



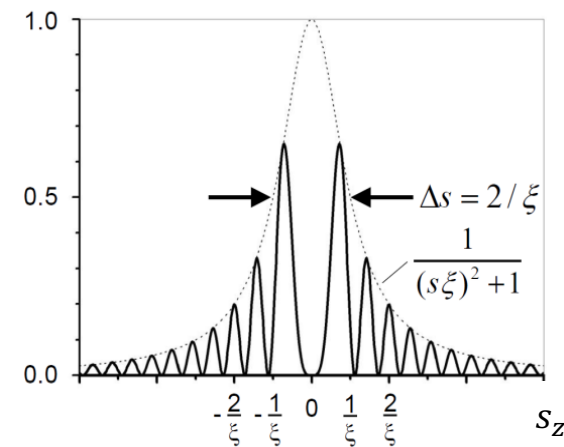
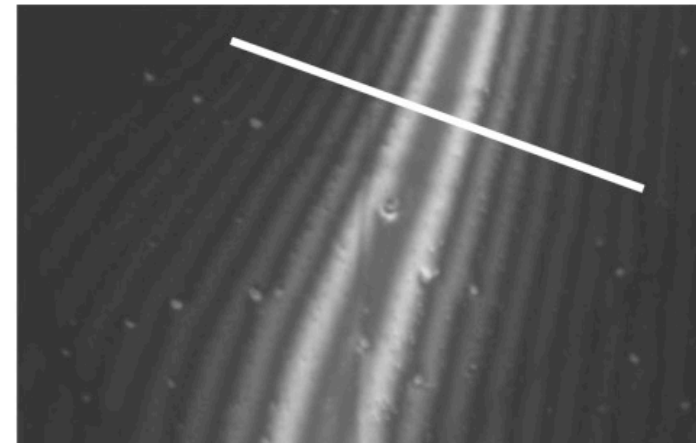
4.3 Contrasts in perfect (single) crystals

Kinematic bending contour
(-400) DF (thin sample point)



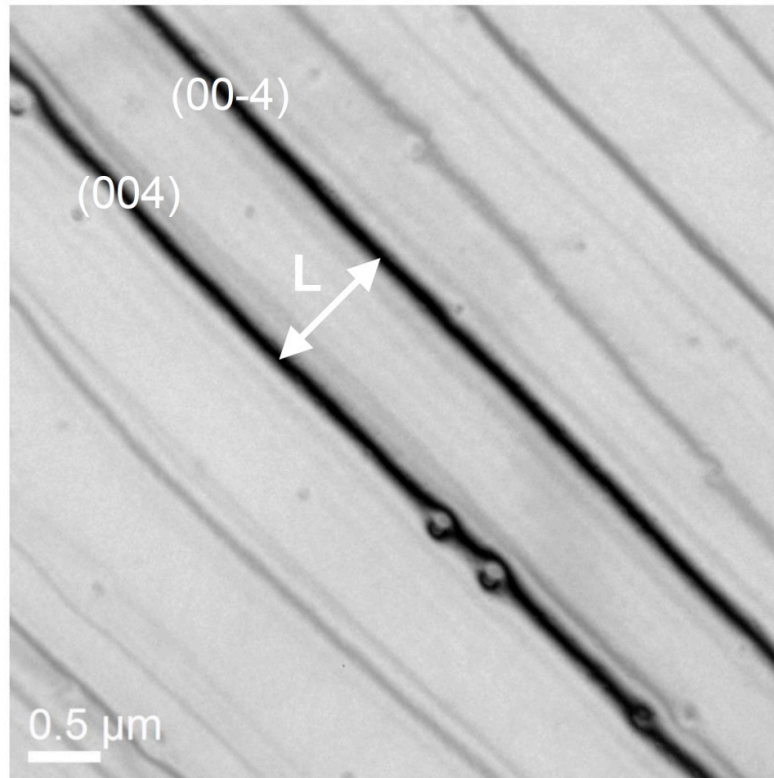
Well described by
$$I_g \propto \frac{\sin^2(\pi \bar{s}_z t)}{(\pi \bar{s}_z)^2}$$

Dynamic bending contour
(-400) DF (thick sample point)



Contradicts
$$I_g \propto \frac{\sin^2(\pi \bar{s}_z t)}{(\pi \bar{s}_z)^2}$$

4.3 Contrasts in perfect (single) crystals

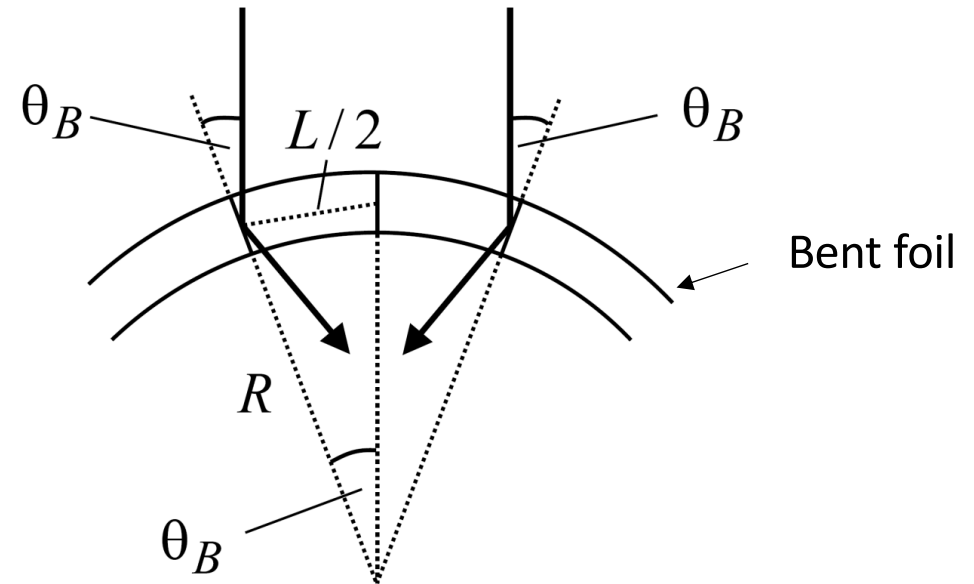


$$L = 985 \text{ nm}$$

$$d_{004} = 0.25 \cdot a_{\text{Si}} = 0.13575 \text{ nm}$$

$$\lambda = 0.00198 \text{ nm}$$

$$\rightarrow R \approx 68 \mu\text{m}$$



$$\sin \theta_B = \frac{L/2}{R}$$

and

$$2d \sin \theta_B = \lambda$$

(Bragg condition)

Radius of curvature:

$$R = \frac{L \cdot d}{\lambda}$$

4.3 Contrasts in perfect (single) crystals

Kinematic theory

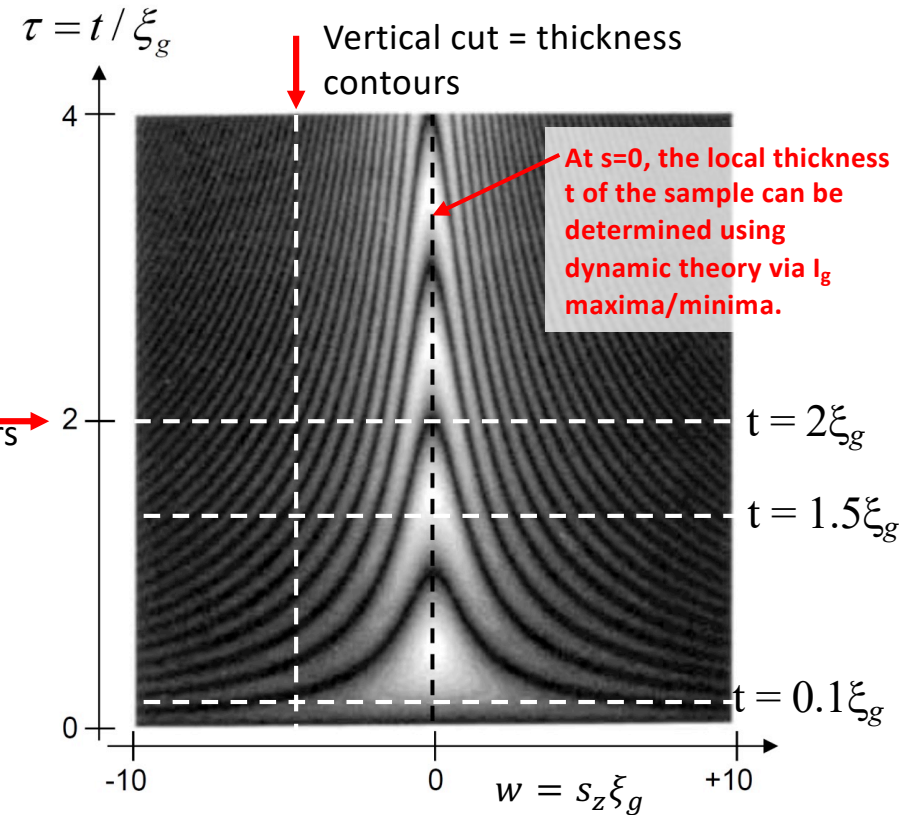
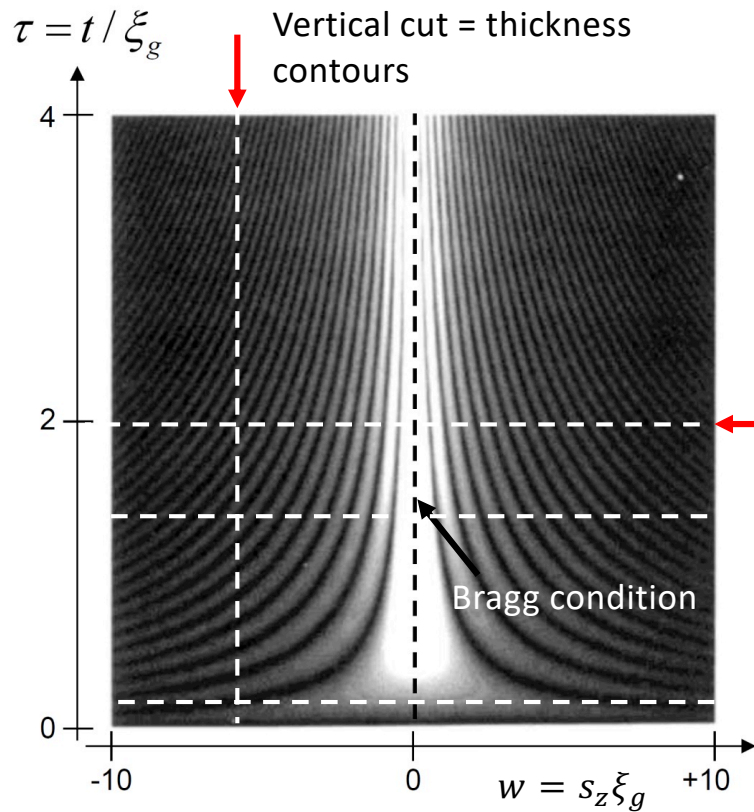
$$I_g \propto F_S^2 \frac{\sin^2(\pi\tau w)}{w^2}$$

vs.

dynamic theory

$$I_g \propto F_S^2 \frac{\sin^2(\pi\tau\sqrt{1+w^2})}{w^2+1}$$

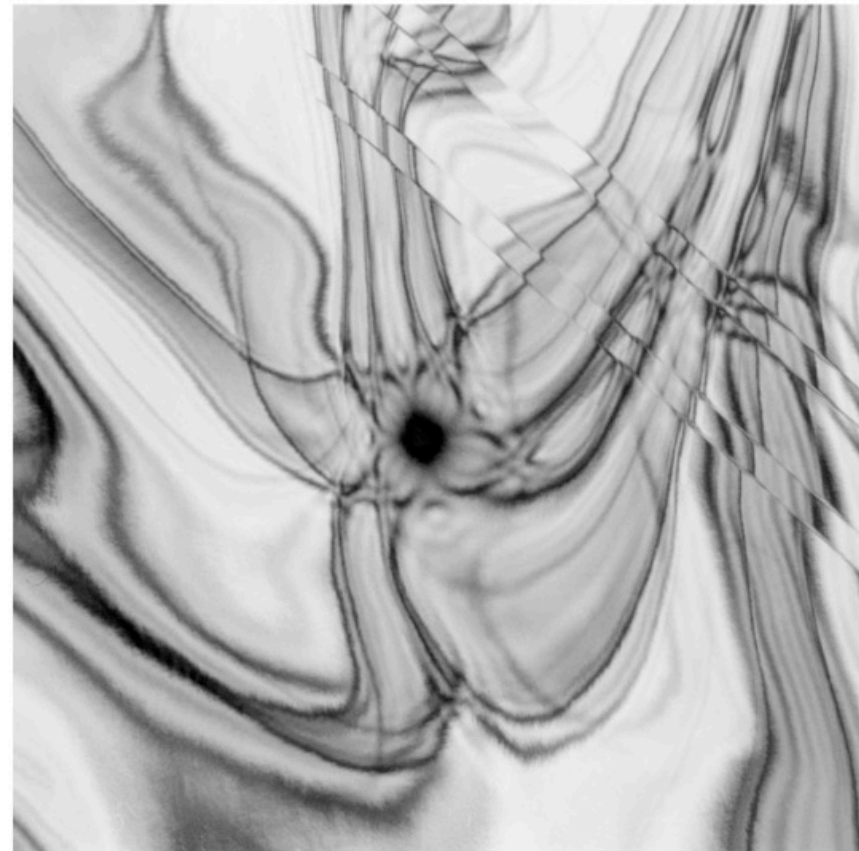
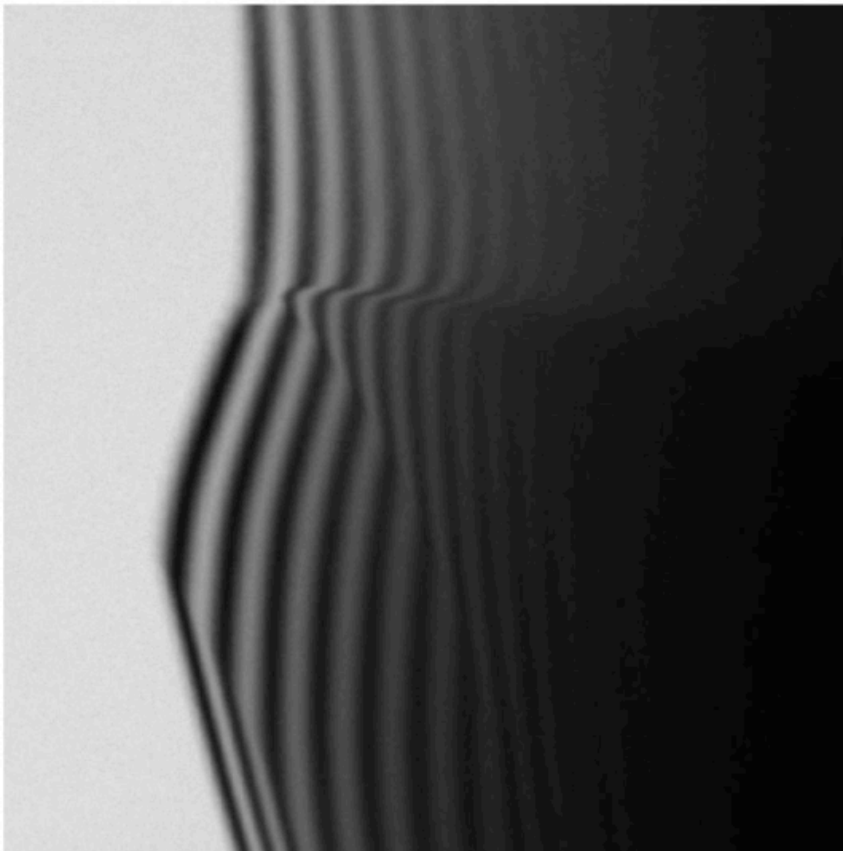
$$w \rightarrow \sqrt{1+w^2}$$



Kinematic theory is a good approximation for $w \gg 1$ and/or $t \ll \xi_{g,eff}$

4.3 Contrasts in perfect (single) crystals

Contrasts in the perfect crystal: thickness and bending contours



Determination of local specimen thickness and specimen curvature based on thickness contours and bending contours.

4.3 Contrasts in perfect (single) crystals

- The reciprocity theorem describes conditions under which STEM and TEM images show identical contrast. In TEM, an objective aperture is used in the back focal plane to isolate certain reflections which are then used to generate the (BF/DF) image. In STEM, an electron ring detector is used to detect the scattered electron intensity signal for each grid point in the sample.
- Mass-thickness contrast: Is a change in intensity that occurs due to more strongly scattering areas (e.g. foreign phases) in the sample or an increase in sample thickness. A pure mass contrast (atomic scattering factor) is only present in amorphous samples (without elastic scattering effects), often the case in biological samples.
- Column approximation is used to calculate I_g and I_0 using kinematic or dynamic diffraction theory for the relevant sample thickness t , imaging vector g and excitation error s .
- Kinematic description of the intensity of the deflected beam: $I_g = F_S^2 G^2 \propto F_S^2 \frac{\sin^2(\pi s_z t)}{(\pi s_z)^2}$
- With const. Deviation parameter s as a function of the sample thickness results in a simple \sin^2 dependency. With periodic zeros at a distance of $1/s$. I_0 and I_g are complementary.
- Kinematic description only fulfilled if $s \gg 0$. According to the kinematic theory, no thickness contours are expected in the Bragg condition ($s=0$), but some are observed experimentally, therefore the application of the dynamic theory is necessary.
- Result of the dynamic diffraction theory: Formally identical to the result of the kinematic diffraction theory. Replacement of s_z by **effective excitation error**: $\bar{s}_z = \sqrt{s_z^2 + \frac{1}{\xi_g^2}}$
- If $s \neq 0$, but still not so large that the requirements of the kinematic theory are met, we use the following for the effective extinction length: $\xi_{g,eff} = \frac{1}{s_z} = \frac{\xi_g}{\sqrt{1+w^2}}$ and introduce a deviation parameter, which represents a normalized excitation error. With dynamic theory and characteristic extinction length, sample thickness at $s=0$ can be determined via the intensity minima or maxima of the thickness contours.
- Bending contours (const. t and change of s): Frequently occurring contrast phenomenon in crystalline samples: Formation of bending contours in areas where the bending condition is locally fulfilled due to the bending of the sample. They help to roughly adjust for certain crystallographic orientations.
- The sample curvature can be determined via bending contours.